Parametric investigation of a humidification dehumidification desalination system with open-air and semi-closed seawater configurations powered by waste heat

W.F. He*, J.J. Chen, D. Han

Nanjing University of Aeronautics and Astronautics, College of Energy and Power Engineering, No. 29 Yudao Street, Qinhuai District, Nanjing, Jiangsu Province, 210016, China, Tel./Fax +8602584893666, email: wfhe@nuaa.edu.cn, wfenghe@polyu.edu.hk (W.F. He)

ABSTRACT

Humidification dehumidification processes have been extensively introduced to the field of desalination. In this paper, a water-heated humidification dehumidification desalination system (HDDS), with open-air and semi-closed seawater water configurations, is proposed to achieve the waste heat recovery. After establishing the energetic and entropic equations of the humidification dehumidification desalination system, the corresponding analysis is accomplished. Furthermore, the dependence of the desalination performance, including the water production and relevant thermal efficiency, to the effectiveness, and cycle ratio are focused. The simulation results show the peak values of water production and gained-output-ratio (GOR) emerge at the balance condition of the humidifier. Nevertheless, due to the acquisition of the negative entropy generation rate, the actual values of water production and GOR are found as 104.64 kg h^{-1} and 1.98. Based on the parametric analysis, it is found that a lower humidification effectiveness is beneficial to raise the actual desalination performance, while the HDDS performance will be elevated after the increase of the dehumidification effectiveness. Furthermore, the improvement of energy conversion for the current configuration is also proved in response to recover partial brine into the feed seawater.

Keywords: Humidification–dehumidification; Desalination; Waste heat recovery; Gained-output-ratio; Effectiveness; Cycle ratio

1. Introduction

Owing to the serious pollution from the industrial discharge, water shortage is more and more serious all over the world. As a result, kinds of desalination methods, which were applied to produce water from seawater or brackish water, were advised and taken into reality in the past decades [1,2]. Nevertheless, the existing desalination systems, including the multi-stage flashing (MSF), multi-effect distillation (MED), vapor compression and membrane type [3–6], are always appropriate for the occasions with large scale water requirement, complicated configuration, huge energy consumption and investment are the main short-

comings. However, small scale water requirement with much more efficient thermal processes are also urgent to be investigated. A very promising desalination type, with humidification dehumidification as the core processes was proposed and developed [7–10], and extensive investigations have been accomplished on such method in the field of desalination.

After building the mathematical models for the different HDDS, Narayan [11] focused on the simulation for the relevant performance based on the software of Engineering Equation Solver (EES). Moreover, further specific methods were advised to update the initial desalination systems, containing varied pressure using mechanical or thermal vapor compression [12,13] and extraction and injection [14]. It was found that the aforementioned propos-

*Corresponding author.

als were verified to be effective to improve the efficiency during the production. Campos [15] built a mathematical models considering saturated air cycling within the water-heated HDDS, with closed-air, open-water configurations. Through the established experimental platform, four critical parameters were prescribed to minimize the summation of the squared residuals for the obtained temperature values. After validating the mathematical models, a sensitive analysis from input and project parameters on the water production was executed. It was found that the absorbed heat from the solar heater, the humidifier height and the mass flow rate of the seawater were the most significant factors to impact the desalinated water production, while the corresponding influences from the environment temperature is very limited. In the recent years, different humidification dehumidification configurations were gradually proposed to investigate the relevant performance. Al-Sulaiman [16] using a solar collector with parabolic trough to heat the cycling air in the HDDS. Thermodynamic performance of the HDDS was first obtained, and the impact principles from the layout of the collector on the HDDS performance were also focused. It was proved that the used solar collector was very suitable to the air-heated HDDS, especially for the configurations with the air heater placed between the humidifier and dehumidifier. Chehayeb [17] achieved the thermodynamic balancing for single and two-stage water-heated HDDS with closed-air, open-seawater configurations, and the humidifier was filled by packings and a bubble column was applied in the dehumidifier. The laws of the flow rate ratio to influence the system entropy generation and forces of heat and mass transfer (HMT) processes were revealed. Based on the modified definition of energy effectiveness, the air extraction and injection were applied to enhance the performance of the HDDS, and the improvement effect and relevant mechanism were investigated. In view of the abundant waste heat in the industry, it was also a good candidate to drive the HDDS. He [18,19] investigated the waste heat powered water-heated and air-heated HDDS, with closed-air, open-seawater configurations. Based on the built mathematical models, the thermodynamic performance of the HDDS was first calculated. Once acquiring all the thermodynamic parameters within the system, the specific scales of all the involved components were determined, and then the economic performance of the HDDS was also obtained.

In addition of the thermodynamic analysis on the basis of first law, it was advised that the relevant calculation is also necessary to confirm the feasibility of the studied objective based on the second law. Mistry [20] achieved the calculation of entropy generation within a HDDS with closed-air and open-water configurations, and both the air and water heaters were placed. The balance equations both for the exergetic and entropy generation were built. After the simulation results were gained, it was suggested that the minimization analysis for the entropy generation was important and useful to determine the critical components and the relevant operation conditions, which should be taken into consideration during the designing process of the HDDS. A packed bed dehumidifier was introduced into the HDDS driven by waste heat by He [21]. The coupled relations between the HDDS and the waste heat source were demonstrated. In accordance with the established conservation equations, thermodynamic simulation was completed to present the desalination performance, in combination with the value of entropy generation rate to judge the possibility of the applied thermal parameters.

The aforementioned literature indicated that the present investigations involved in the HDDS mainly focus on the configurations with open-seawater type, in which the cycle of the seawater is open. Narayan [22] mentioned a new type of the HDDS with closed-seawater, open-air structure, and it was pointed out that when high efficiency humidification and optimal operating conditions are applied, this kind of system is more productive than the general open-water version. An open-air solution system to achieving evaporation with a more rigorous mathematical model for the humidification process was proposed by Huang [23]. After building the programmes of the performance simulation for the entire system, the influences from thermal parameters on the evaporation load and energy conversion efficiency were explored through the theoretical simulation. It was discovered that the inlet temperature as well as the reflux ratio of the solution into the humidification process was proportional to the evaporation load. As a result, the optimization method was involved to maximize the evaporation capacity, with a suitable air mass flow rate. Mahdizade [24] proposed a semi-open air, open-water humidification dehumidification desalination unit to produce water. The obtained results showed that the suggested method was effective to enhance the water producing performance at fixed top temperatures for dual heating processes both for water and air.

Hence, it can be concluded that a very small number of works in literature consider the HDDS with the open-air and semi-closed seawater configurations. The detailed thermodynamic analysis of the open-air and semi-closed seawater HDDS, especially the heat recovery mechanisms with the original brine cycled into the feed stream, should be explored, and the practicability criteria through the calculation of the entropy generation rate of the thermal components should also be achieved. In the present paper, the open-air and semi-closed seawater configurations are conducted to enhance the performance of the water-heated humidification dehumidification desalination method, with the waste heat driving the whole system. The mathematical models, aiming to achieve the energy and entropy analysis was established. In addition of the performance for the HDDS at the designed input conditions, the correlation between the characteristics of the desalination system and the effectiveness of the core components, and the cycled ratio are also calculated. The research results provide significant references for the design and further optimization of the HDDS.

2. Description of the HDDS with open-air and semi-closed seawater configurations

The schematic diagram of the HDDS, with open-air and semi-closed seawater configurations is presented in Fig. 1. It is found that the HDDS consists of the humidifier with packings, dehumidifier, the waste heat recovery exchanger (WHRE). Different from the general configuration with the closed-air, open-seawater version, the ambient air first enters
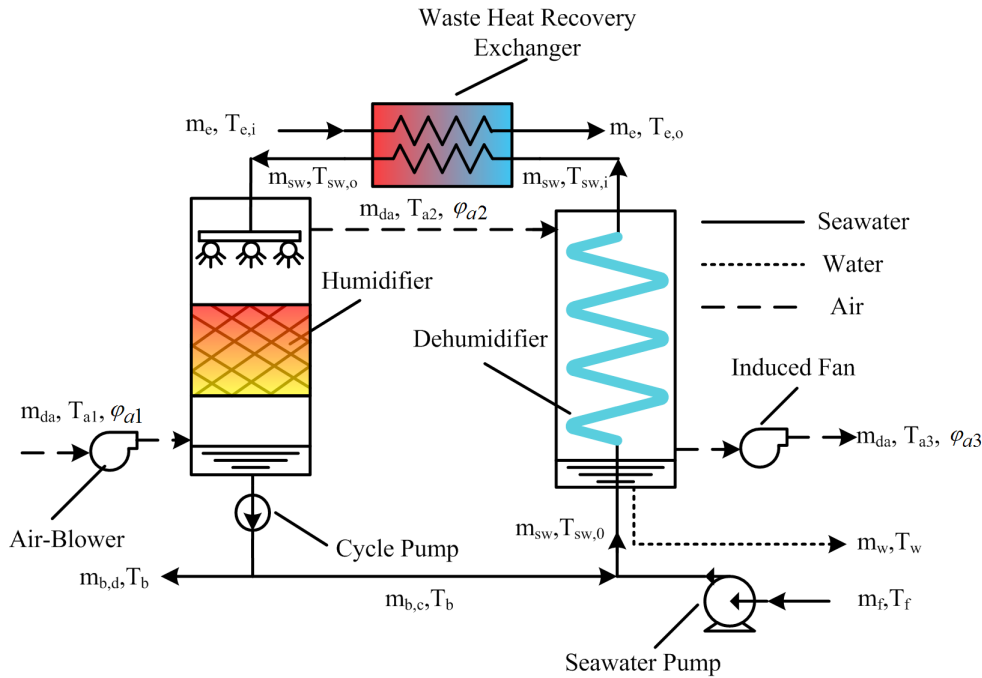
Fig. 1. Configuration schemes of the current HDDS with waste heat recovery.

the humidifier and flows out after the dehumidification, while the seawater stream is closed although the existing of the feed seawater inlet and brine outlet. Actually, the feed seawater joins the concentrated seawater from the bottom of the humidifier to compensate the discharged brine, and then the confluent seawater flows into the surface dehumidifier, absorbing the condensing heat from the saturated and hot humid air. Therefore, the salinity of the seawater into the dehumidifier is higher than that in the general HDDS. After the preheating in the dehumidifier, the seawater temperature arrives at a top value, accomplishing the waste heat recovery in the heat exchanger. Finally, the hot seawater is sprayed into the packings, transferring mass and heat with the ambient air. Accordingly, the seawater concentrates while the ambient is humidified. However, in order to fully recover the energy within the HDDS, part of the brine is recycled into the humidifier to close seawater cycle.

In order to establishing the mathematical equations for all the components in the HDDS, and obtain the corresponding performance successfully, the following assumptions are made during the simulation:

(1) The current HDDS runs at the steady-state conditions.
(2) Energy loss to the surroundings, the kinetic and potential energy changes during the heat transfer processes are neglected.
(3) The humid air after humidification and dehumidification is saturated, as $\phi_{a2} = 1$.
(4) Fouling thermal resistance of the heat and mass transfer devices, including the heat exchangers and packings, are not taken into consideration.
(5) Power consumptions of the pump, blower and fan are ignored.

3. Mathematical models of the HDDS with open-air and semi-closed seawater configurations

3.1. Waste heat recovery exchanger

In order to utilize the waste heat in the industry, a heat exchanger is applied to transfer the energy to the seawater, driving the whole desalination system. Therefore, the hot side within the waste heat recovery exchanger is the gas exhaust, while the cold aspect is the preheated seawater from the dehumidifier. With the arrangement of counter flow, the relevant temperature variation along the length of the exchanger is presented in Fig. 2 (a), and the energy equilibrium equation is calculated in Eq. (1) [25]:

$$Q_{WHRE} = m_{sw} \cdot (h_{sw,o} - h_{sw,i}) = m_e \cdot (h_{e,i} - h_{e,o}) \qquad (1)$$

Actually, in addition of the energetic analysis for the heat exchanger, the entropy equation during the heat transfer process is also necessary to reveal the irreversible loss, and the relevant entropy generation rate of the WHRE, $S_{gen, WHRE}$ is expressed as follows:

$$S_{gen,WHRE} = m_{sw}(s_{sw,o} \text{-} s_{sw,i}) + m_e(s_{e,o} - s_{e,i}) \qquad (2)$$

3.2. Direct contact humidifier with packings

To evaporate the carried water in the seawater, packings are applied to fill the humidifier, providing the space for HMT between the inflow seawater and humid air. Actually, the preheated seawater is sprayed into the humidifier and contact with the conducted ambient air directly, with the psychrometric chart in Fig. 2(b). The corresponding mass and energy balance equations during the humidification are respectively gained as [26]:

(a) WHRE

(b) Psychrometric chart of humid air
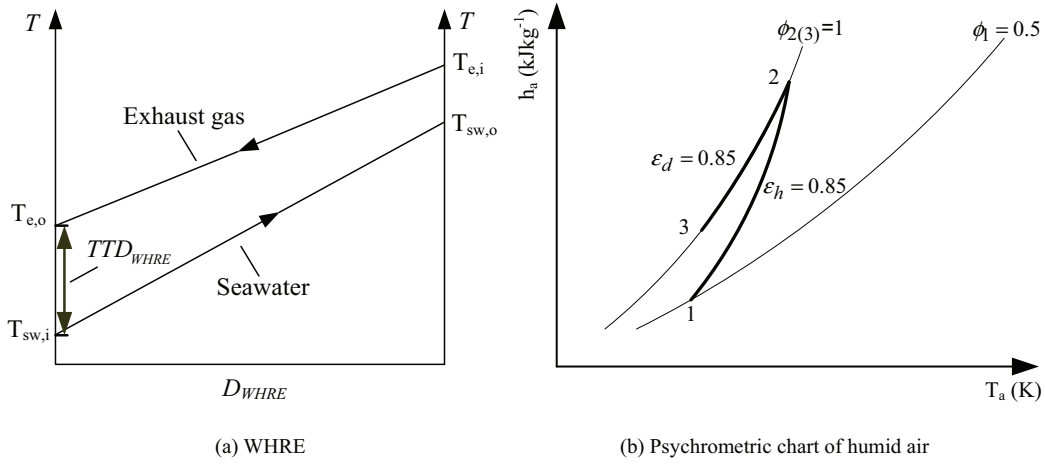
Fig. 2. Temperature profiles and the psychrometric chart within the HDDS with open-air and semi-closed seawater configurations.

$$m_{sw} - m_b = m_{da}(w_2 - w_1) \tag{3}$$

$$m_{sw}h_{sw,o} - m_b h_b = m_{da}(h_{a2} - h_{a1}) \tag{4}$$

As the core component of the HDDS, the characteristics of the humidifier is especially significant for the water production capacity. Consequently, the definition of effectiveness is provided to measure the macroscopical conditions during the mass and heat transfer between the seawater and humid air, presented in Fig. 2(b), and the specific equation is expressed as follows [27]:

$$\varepsilon_h = \frac{\Delta H_h}{\Delta H_{h,\max}} \tag{5}$$

The detailed expressions of ΔH_h can be given as:

$$\Delta H_h = m_{sw}h_{sw,o} - m_b h_b = m_{da}(h_{a2} - h_{a1}) \tag{6}$$

With respect to the value of $\Delta H_{h,max}$, the specific expression both for the seawater and air sides are listed in Eqs. (7) and (8).

$$\Delta H_{h,\max,sw} = m_{sw}h_{sw,o} - m_{b,a1}h_{b,a1} \tag{7}$$

$$\Delta H_{h,\max,a} = m_{da}(h_{a,sw,o} - h_{a1}) \tag{8}$$

Hence, the actual value of $\Delta H_{h,max}$ can be obtained as:

$$\Delta H_{h,\max} = \min(\Delta H_{h,\max,sw}, \Delta H_{h,\max,a}) \tag{9}$$

At the aspect of the entropy equation, the related entropy generation rate during the humidification, $S_{gen,h}$, can be acquired by Eq. (10).

$$S_{gen,h} = m_b s_b - m_{sw} s_{sw,o} + m_{da}(s_{a2} - s_{a1}) \tag{10}$$

3.3. Surface type dehumidifier

In the current desalination system, surface type dehumidifier is applied to condense the humidified hot air, and thus the pure water can be produced. Accordingly, the corresponding mass and energy equilibrium are acquired as:

$$m_w = m_{da}(w_2 - w_3) \tag{11}$$

$$m_{sw}(h_{sw,i} - h_{sw,0}) = m_{da}(h_{a2} - h_{a3}) - m_w h_w \tag{12}$$

Similar to the humidification, effectiveness is also defined to characterize the comprehensive performance of the heat transfer process in the dehumidifier, exhibited in Fig. 2(b), and the specific expression can be calculated as follows [27]:

$$\varepsilon_d = \frac{\Delta H_d}{\Delta H_{d,\max}} \tag{13}$$

The specific expression of ΔH_d is listed as:

$$\Delta H_d = m_{sw}(h_{sw,i} - h_{sw,0}) = m_{da}(h_{a2} - h_{a3}) - m_w h_w \tag{14}$$

where h_w is the specific enthalpy of the produced water, and it is assumed that the obtained water is saturated at the average of the inlet and outlet temperature for the humid air.

For the aspect of $\Delta H_{d,max}$, the detailed equations for the seawater and humid air can be calculated in Eqs. (15) and (16).

$$\Delta H_{d,\max,sw} = m_{sw}(h_{sw,a2} - h_{sw,0}) \tag{15}$$

$$\Delta H_{d,\max,a} = m_{da}(h_{a2} - h_{a,sw,0}) - m_{w,sw,0}h_{w,sw,0} \tag{16}$$

Hence, the actual value of $\Delta H_{h,max}$ can be obtained as:

$$\Delta H_{d,\max} = \min(\Delta H_{d,\max,sw}, \Delta H_{d,\max,a}) \tag{17}$$

Additionally, the same as the humidification, the corresponding entropy generation rate, $S_{gen,d}$ can be calculated as:

$$S_{gen,d} = m_{sw}(s_{sw,i} - s_{sw,0}) + m_{da}(s_{a3} - s_{a2}) + m_w s_w \tag{18}$$

3.4. Mixing process between the feed seawater and the recycled brine

In order to elevate the energy utilization efficiency within the desalination system, part of the discharged brine is recycled into the feed seawater, and then the mixed seawater flows into dehumidifier to condense the hot and saturated humid air. Hence, for the mixing process, the related mass, salinity and energy balance equations can be obtained as:

$$m_{sw} = m_f + m_{b,c} \tag{19}$$

$$m_{sw}h_{sw,0} = m_f h_f + m_{b,c} h_b \tag{20}$$

In addition of the mass and energetic analysis, the entropy generation rate during the mixing process can be calculated as:

$$S_{gen,mix} = m_{sw}s_{sw,0} - m_{b,c}s_b - m_f s_f \tag{21}$$

Furthermore, the cycled ratio is defined to express the relation between the mass flow rate of the feed seawater and cycled brine.

$$CR = \frac{m_{b,c}}{m_f} \tag{22}$$

3.5. Assessment of the HDDS with open-air and semi-closed seawater configurations

Besides the production of the HDDS, thermal efficiency is also the focus to appraise the corresponding energy conversion status. Accordingly, GOR is used to indicate the situation of energy utilization.

$$GOR = \frac{m_w h_{fg}}{m_e \cdot (h_{e,i} - h_{e,o})} \tag{23}$$

Moreover, after the entropy generation rate of the included thermal processes are calculated, the total entropy generation rate and the specific entropy generation rate of the water production can be summarized as:

$$S_{gen,t} = S_{gen,d} + S_{gen,h} + S_{gen,WHRE} + S_{gen,mix} \tag{24}$$

$$s_{gen,t} = \frac{S_{gen,t}}{m_w} \tag{25}$$

Consequently, the mathematical models of the HDDS with open-air and semi-closed seawater configurations are analyzed, and the performance simulation can be completed through the Matlab platform with the established equations iteratively solved.

4. Validation of the HDDS with open-air and semi-closed seawater configurations

In order to guarantee the accuracy of the acquired results for the proposed HDDS, the initially built mathematical

Table 1
Typical thermodynamic parameters of the HDDS

S (g/kg)	35
ε_h	0.85
ε_d	0.85
ϕ_{a1}	0.5
ϕ_{a2}	1
ϕ_{a3}	1
CR	5
$T_{sw,0} = T_{a1}$ (K)	303.15
$T_{sw,o}$ (K)	353.15
TTD_{WHRE} (K)	10

Table 2
Thermal conditions of the waste heat source

Term	Value
$T_{e,I'}$ K	383.15
$m_{e,}$ kg/s	1.0
Mole fraction	
CO_2, %	41.2
N_2, %	58.8

models must be fully validated. Due to the kernel effect in the system, the humidification and dehumidification performance is simulated and contrasted with the published results from G. P. Narayan [28] at the same input conditions. The relevant comparisons of the component performance between the current HDDS and that in the reference are shown in Table 3 and Table 4, respectively. It is observed that the maximum error for the humidification process is 0.28% for the mass flow rate of the concentrated brine, while the corresponding maximum error for the dehumidification appears with a value of 5.1% for the condensed water. The small errors of the two core processes verify the accuracy of the established mathematical models.

5. Results and discussion

In accordance with the mass, energy and the entropy equations, characteristics of the HDDS are initially calculated at different air mass flow rate at the designed input conditions, shown in Table 1. It is seen that effectiveness both for the humidifier and dehumidifier are assumed as $\varepsilon_h = 0.85$ and $\varepsilon_d = 0.85$, while the terminal temperature difference of the WHRE are fixed at $TTD_{WHRE} = 10$ K. Waste heat reserved in the exhaust gas with thermodynamic parameters shown in Table 2, is applied as the driven power, raising the seawater temperature sprayed into the humidifier.

5.1. Performance analysis of the HDDS at designed conditions

In the current HDDS, the open-air and semi-closed seawater scheme is applied, and the discharged brine is cycled into the feed seawater to recover the relevant carried internal energy. Based on the definition of effectiveness for the humid-

Table 3
Comparison of the humidification performance between the current HDDS and that of Narayan [28]

Term	ε_h	m_{sw} (kg s^{-1})	m_{da} (kg s^{-1})	$T_{sw,o}$ (K)	T_{a1} (K)	Φ_1	Φ_2	T_{a2} (K)	m_b (kg s^{-1})	T_b (K)
Simulation	0.9	0.15	0.1	335.94	307.35	1	1	324.05	0.14	310.31
Narayan [28]	0.9	0.15	0.1	335.94	307.35	1	1	324.55	0.14	310.20
Error(%)	–	–	–	–			–	0.15	0.28	0.04

Table 4
Comparison of the dehumidification performance between the current HDDS and that of Narayan [28]

Term	ε_d	m_{sw} (kg s^{-1})	m_{da} (kg s^{-1})	$T_{sw,0}$ (K)	T_{a2} (K)	Φ_2	Φ_3	T_{a3} (K)	m_w (kg h^{-1})	$T_{sw,i}$ (K)
Simulation	0.9	0.15	0.1	303.15	363.15	1	1	307.17	20.16	335.62
Narayan [28]	0.9	0.15	0.1	303.15	363.15	1	1	307.35	21.24	335.94
Error(%)	–	–	–	–			–	0.06	5.1	0.1

(a) Humidifier
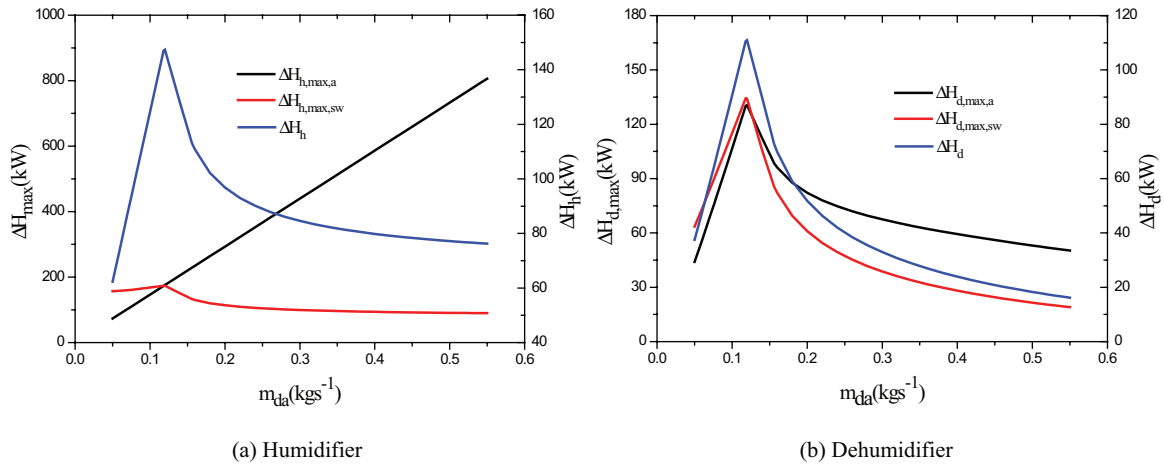
(b) Dehumidifier

Fig. 3. Maximum total enthalpy difference and corresponding actual enthalpy difference for the heat and mass exchanger.

ification and dehumidification, the corresponding calculation process and results are presented in Fig. 3. As the result from the minimum value of the maximum total enthalpy difference, ΔH_{max}, multiplying the effectiveness, ε, it is found that there exists a break point at the variation curve of the actual total enthalpy difference, ΔH, both for the humidification and dehumidification. In reality, with the increase of the air mass flow rate, the variation laws of the maximum total enthalpy change is different for the two kinds of involved fluid. Taking the humidification into consideration in Fig. 3a, it is obvious that the value of $\Delta H_{h,max,a}$ rises from $\Delta H_{h,max,a} = 73.28$ kW at $m_{da} = 0.05$ kg s^{-1} to $\Delta H_{h,max,a} = 806.13$ kW at $m_{da} = 0.55$ kg s^{-1}, while the relevant value of $\Delta H_{h,max,sw}$ first rises to $\Delta H_{h,max,sw} = 173.43$ kW until $m_{da} = 0.12$ kg s^{-1} and then descends to $\Delta H_{h,max,sw} = 89.74$ kW at $m_{da} = 0.55$ kg s^{-1}. Consequently, the intersection emerges at $m_{da} = 0.12$ kg s^{-1}, which is called as the balance condition of the humidifier with the relation of $\Delta H_{h,max,a} = \Delta H_{h,max,sw}$. With the switch of the maximum total enthalpy difference for the two kinds of the involved working fluid at the balance condition of the humidifier, the peak value of $\Delta H_h = 147.01$ kW arises with the expression of $\Delta H_{h,max,a} = \Delta H_{h,max,sw}$.

With respect to the dehumidification in Fig. 3(b), it is observed that the turning point arises at the variation curve

for the maximum total enthalpy difference, $\Delta H_{d,max}$, as well as the actual enthalpy difference, ΔH_d. Nevertheless, different from the change laws for the humidification, the peak value of the maximum total enthalpy difference emerges at the case of $\Delta H_{h,max,a} = \Delta H_{h,max,sw}$ while the relevant intersection point is discovered at the case of $\Delta H_{d,max,a} = \Delta H_{d,max,sw}$. As a result, the corresponding top value of the actual total enthalpy change, $\Delta H_d = 110.64$ kW, is found at the case $m_{da} = 0.12$ kg s^{-1}. In view of the turning effect at the case of $\Delta H_{h,max,a} = \Delta H_{h,max,sw}$, it can be inferred that all the parameters will be influenced due to the application of the actual enthalpy difference, ΔH, during the simulation processes. In fact, the final utilization of ΔH is reasonable because the maximum values of the peak total enthalpy difference at the ideal conditions is impossible to be approached.

After the values of ΔH both for the humidifier and dehumidifier are calculated based on the definition of effectiveness, all the variables within the HDDS can be acquired, and the relevant trends will be influenced, especially at the balance condition of the humidifier with top values of ΔH. Different mass flow rate and the temperature values with the increase of the air mass flow rate are presented in Fig. 4. It is found in Fig. 4a that the maximum value of the feed

(a) Mass flow rate   (b) Temperature
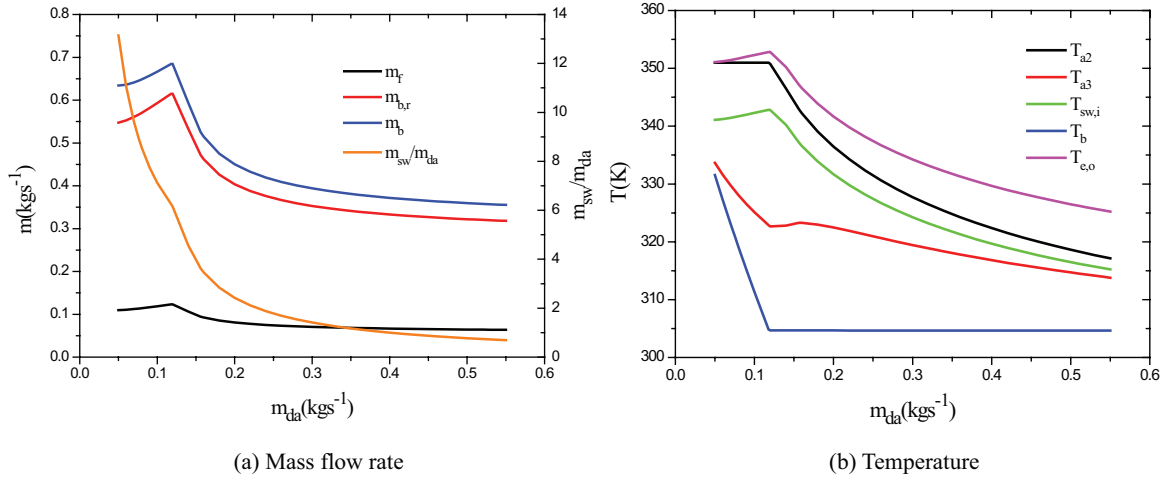
Fig. 4. Critical parameters within the HDDS.

seawater and cycled brine is m_f = 0.12 kg s^{-1} and $m_{b,r}$ = 0.61 kg s^{-1}, respectively, at the balance condition of the humidifier. Therefore, the corresponding maximum seawater mass flow rate involved in the humidification and dehumidification processes, obtained as the accumulation of the feed seawater and the cycled concentrated brine, is calculated at m_{sw} = 0.74 kg s^{-1}. It was proved that the mass flow rate ratio between the seawater and humid air is especially critical for the performance of the HDDS, and the relevant value is calculated to decline continuously from m_{sw}/m_{da} = 13.14 at m_{da} = 0.05 kg s^{-1} to m_{sw}/m_{da} = 0.69 at m_{da} = 0.55 kg s^{-1}. As a result, with the declination of the mass flow rate ratio, the outlet air temperature during the humidification process, T_{a2}, decreases from T_{a2} = 350.97 K at m_{da} = 0.05 kg s^{-1} to T_{a2} = 317.14 K at m_{da} = 0.55 kg s^{-1}, shown in Fig. 4b, and the temperature of the discharged humid air, T_{a3}, also drops from T_{a3} = 333.65 K to T_{a3} = 313.79 K in succession. Furthermore, with respect to the outlet temperature of the exhaust gas, it can be seen that the corresponding variation law is consistent to that for the temperature of the preheated seawater during dehumidification at the fixed top temperature of the seawater, with a top value of $T_{e,o}$ = 352.81 K at the balance condition of the humidifier.

In correspondence with the variation laws of the air temperature within the HDDS, the humidity ratio can be obtained easily. In combination with the assumption of the fixed relative humidity, the relevant humidity ratio of the humid air before and after the dehumidification process in Fig. 5. It is seen that the length sandwiched in the humidity ratio curves first expands to Δω = 0.38 kg kg^{-1} until the balance condition of the humidifier, and then it falls to the minimum value of Δω = 0.01 kg kg^{-1} at m_{da} = 0.55 kg s^{-1}. Consequently, the water production of the desalination system can be calculated by the dry air mass flow rate multiplying the humidity ratio difference, and it is obtained that the peak water production appears with a value of m_w = 162.04 kg h^{-1} at the case of m_{da} = 0.12 kg s^{-1}.

It has been stated that the waste heat is applied to drive the desalination system, heating the preheated seawater from the dehumidifier, and the recovered heat is just the input energy. Hence, the recovery effect of the waste heat is closely connected to the performance of the HDDS, pre-
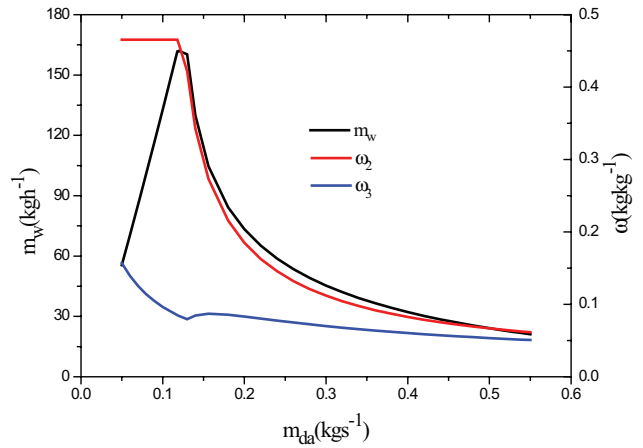
Fig. 5. Water production of the HDDS with the increase of the air mass flow rate.

sented in Fig. 6. Corresponding to the variation laws of the seawater inlet temperature into the WHRE and relevant mass flow rate, it was discovered that there is a bottom value of Q_{WHRE} = 30.04 kW at the balance condition of the humidifier. Due to the fixed mass flow rate and inlet temperature of the waste heat source, a peak outlet temperature of the exhaust gas flowing out of the WHRE is attained at $T_{e,o}$ = 352.81K, shown in Fig. 4b. After the water production and input energy are achieved, the thermal efficiency of the HDDS, which is gain-output-ratio, can be spontaneously achieved as the latent heat to evaporate the gained water divided by the input energy. Finally, the magnitude of GOR ascends to GOR = 3.52 until m_{da} = 0.12 kg s^{-1}, and then it drops to GOR = 0.25 at m_{da} = 0.55 kg s^{-1}.

5.2. Entropy analysis of the HDDS at designed conditions

Distinctly, the previous results of the energetic analysis makes clearly the heat transfer and energy conversion conditions within the desalination system. However, the entropy analysis is also important to appraise the possibil-
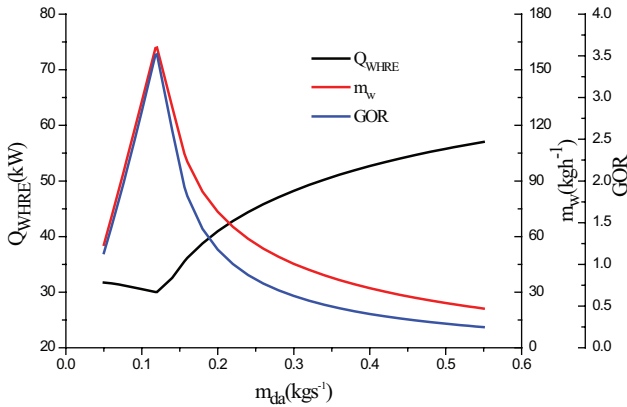
Fig. 6. Energy conversion status within the HDDS with the air mass flow rate.
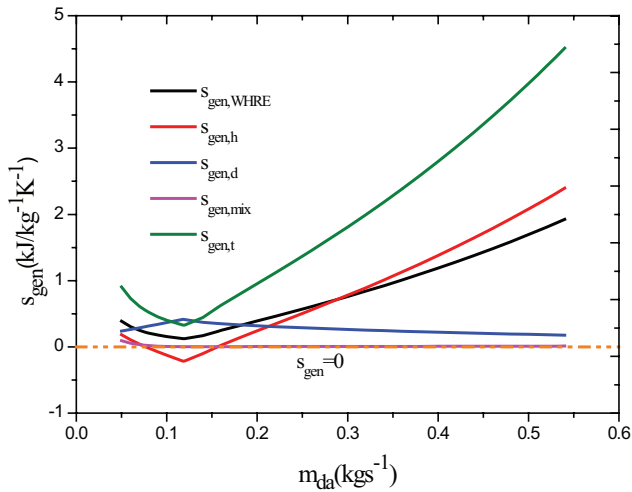
Fig. 7. Specific entropy generation within the HDDS with the air mass flow rate.

ity of the thermal system and demonstrate the irreversible lose during all the referred thermal processes. On the basis of the specific entropy generation rate in Eq. (25), the relevant change laws both for the component and whole system with the increase of air mass flow rate is exhibited in Fig. 7. It is seen that the bottom value of the specific entropy generation rate for all the processes are found at the balance condition of the humidifier. However, according to the second law of thermodynamics, a thermal process is impossible to realize if the relevant entropy generation rate is negative. Accordingly, it is found that the specific entropy generation during the humidification is negative at the range of m_{da} = 0.08 kg s^{-1} to m_{da} = 0.16 kg s^{-1}. As a result, the current HDDS can only run successfully under the remaining cases.

Actually, the results from the second law analysis for the HDDS must be considered and merged into the relevant performance simulation. Eliminating the irrealizable conditions, it can be concluded that the true maximum values for the water production and the relevant GOR emerge with m_w = 104.64 kg h^{-1} at the case of m_{da} = 0.16 kg s^{-1} and GOR = 1.98 at the case of m_{da} = 0.08 kg s^{-1}. Furthermore, for the aspect of the total specific entropy generation rate, the bottom value

of $s_{gen,t}$ = 0.33 kJ kg^{-1} K^{-1} declares the smallest irreversible loss, which is corresponding to the irrealizable peak value of GOR, while the actual minimum value of the total specific entropy generation arrives at $s_{gen,t}$ = 0.56 kJ kg^{-1} K^{-1}. Obviously, the specific entropy generation rate of all the components, but not only the value for the whole system should be analyzed to assess the relevant practicability of the HDDS.

5.3. Influences from the effectiveness on the HDDS performance

The aforementioned part presents the thermodynamic analysis of the HDDS at the fixed value of the effectiveness, ε = 0.85, both for the humidifier and dehumidifier. It is illustrated that the value of effectiveness is significant for the performance simulation since the acquisition of all the parameters within the HDDS is attributed to the determination of the actual total enthalpy difference, ΔH. The value of $ε_h$ is first prescribed to investigate the correlation between the performance of the desalination system and the humidification, presented in Fig. 8. Compared to the designed effectiveness of $ε_h$ = 0.85, an elevation amplitude of 9.07%, 14.69 kg h^{-1}, can be attained once the effectiveness is raised to $ε_h$ = 0.9. Taking the impossible cases with negative entropy generation rate into account, the improvement of the water production disappears. On the contrary, it is found that a lower humidification effectiveness is beneficial to raise the true performance of the desalination system. The actual peak water production is elevated slightly from m_w = 104.64 kg h^{-1} at $ε_h$ = 0.85 to m_w = 108.71 kg h^{-1} at $ε_h$ = 0.8, and the actual corresponding value of GOR is raised from GOR = 1.98 to GOR = 2.10, an improvement of 6.06%.

In addition of the effectiveness for the humidification, the corresponding value of the dehumidifier is also appointed to explore the potential to increase the produced water. A higher effectiveness will result in a more efficient condensing process during the dehumidification. As a result, it is observed in Fig. 9 that the effective peak value of water production can be moved from m_w = 104.64 kg h^{-1} at m_{da} = 0.16 kg s^{-1} to m_w = 118.78 kg h^{-1} at m_{da} = 0.17 kg s^{-1} when the designed effectiveness of $ε_d$ = 0.85 is raised to $ε_d$ = 0.9, and the benefit of the GOR elevation is from GOR = 1.98 to GOR = 2.39. Taking the profits from the effectiveness promotion for the humidification and dehumidification into comparison, it is concluded evidently that the characteristics of the HDDS is more dependent on the performance of the dehumidification process.

5.4. Influences from the cycled ratio for the discharged brine on the HDDS performance

In the current HDDS with open-air and semi-closed seawater configurations, partial brine is recovered to the feed seawater, with the purpose to raise the system performance. Consequently, five values of cycled ratio are appointed to investigate the influence extent shown in Fig. 10. With the increasing cycle ratio from CR = 0 to CR = 7, it is found that the negative region of the entropy generation rate will be compressed. For instance, the range of the negative region of the entropy generation rate at CR = 0 varies from m_{da} = 0.06 kg s^{-1} to m_{da} = 0.14 kg s^{-1}, while it is from m_{da} = 0.08 kg s^{-1} to m_{da} = 0.14 kg s^{-1} at CR = 7. Actually, once the cycle ratio increases, both the mass flow rate and concentration of the

(a) Water production   (b) GOR
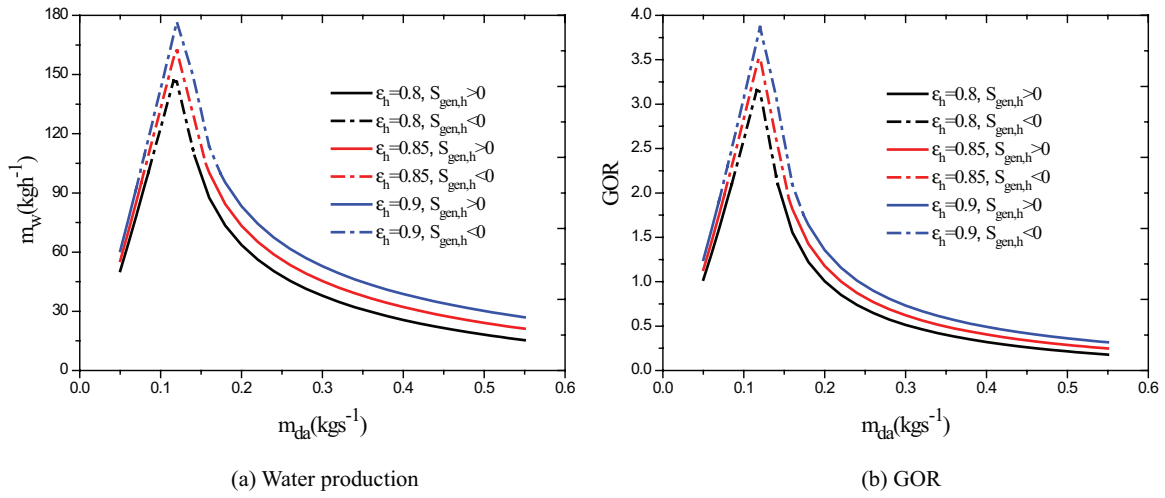
Fig. 8. Performance of the HDDS at different effectiveness of the humidifier.

(a) Water production   (b) GOR
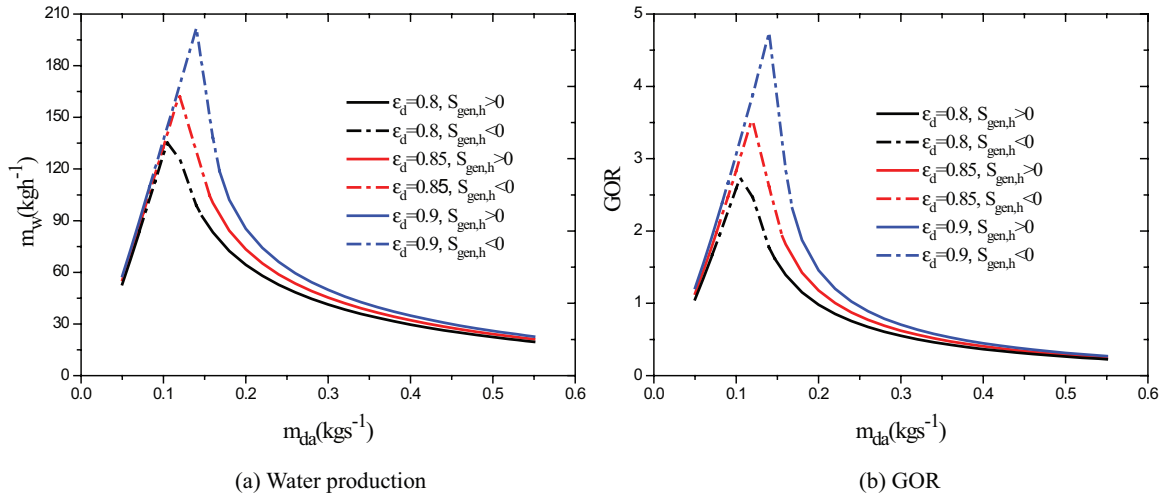
Fig. 9. Performance of the HDDS at different effectiveness of the dehumidifier.

(a) Water production   (b) GOR
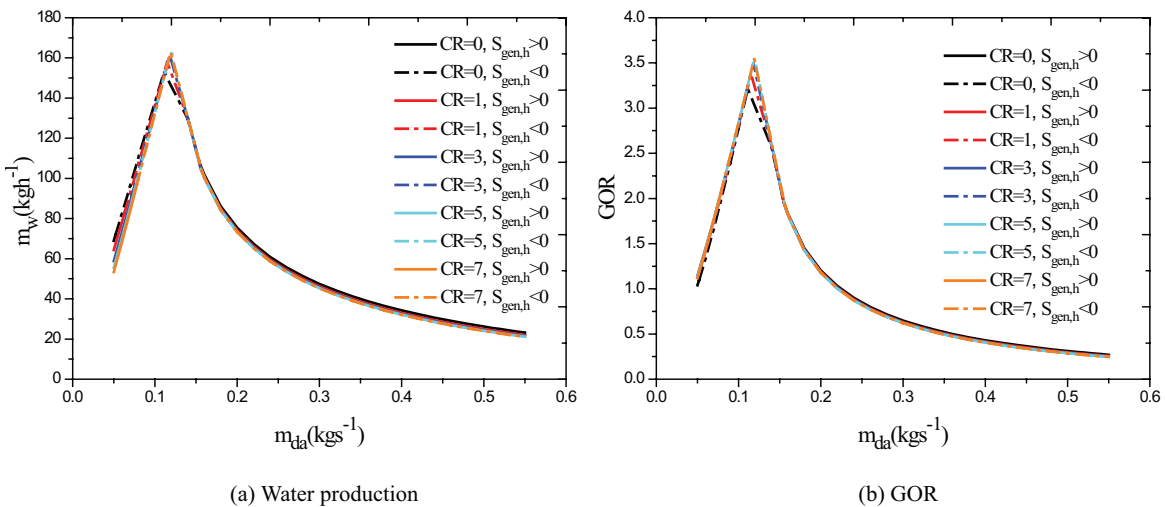
Fig. 10. Performance of the HDDS at different cycled ratios.

seawater into the humidification will rise significantly at the same conditions of the involved air mass flow rate. Furthermore, according to the correlations among the entropy, temperature and concentration [25], it is inferred that the difference of the entropy generation rate for the seawater side during humidification will drops with the increase of the cycle ratio. Finally, the negative region of the entropy generation rate during humidification is compressed.

In addition, compared to the general water-heated HDDS with closed-air and open-seawater configurations, *CR* = 0, it can be found that the current scheme with open-air and semi-closed seawater configurations has advantages to improve the desalination performance. After the gradual elevation of the cycled brine to *CR* = 7, the true top value of GOR is elevated with an amplitude of 4.6%, from *GOR* = 1.96 at m_{da} = 0.16 kg s⁻¹ to *GOR* = 2.05 at m_{da} = 0.08 kg s⁻¹.

6. Conclusions and future work

This paper proposed an humidification dehumidification desalination system, which has the open-air and semi-closed seawater configurations. After the thermodynamic analysis, the detailed results can be concluded given as follows:

1. The balance condition of the humidifier, $\Delta H_{h,max,a}$ = $\Delta H_{h,max,sw}$, is especially significant for the performance of the HDDS owing to the effect from the actual total enthalpy difference during the simulation.
2. The realizable performance of the HDDS can be determined through the combination of energetic and entropy analysis. At the designed conditions, it was found that the true maximum value of the water production emerges as 104.64 kg h⁻¹, and the corresponding thermal efficiency, GOR, arrives at 1.98.
3. A lower humidification effectiveness is beneficial to raise the true desalination performance. The actual peak water production and GOR are elevated slightly from 104.64 kg h⁻¹ and 1.98 to m_w = 108.71 kg h⁻¹ and 2.10, respectively, once the humidification drops from 0.85 to 0.8.
4. The effectiveness elevation of the dehumidifier is more beneficial to raise the performance of the HDDS, and a benefit of 13.51% for the water production and 20.71% for the value of GOR can be obtained, respectively, once the effectiveness is promoted from 0.85 to 0.9.
5. The positive effect on the desalination performance from the cycled brine is proved, with an elevation of 4.6% for the value of GOR.

The current investigation focus on the thermodynamic of the open-air and semi-closed seawater HDDS, and the change laws from the critical parameters on the desalination performance are obtained. In the future research, the economic aspect of the HDDS should be achieved, and the optimization method should also be introduced to determine the best performance as well as the relevant thermal parameters.

Symbols

D_{WHRE}	—	Distance along the WHRE (mm)
h	—	Enthalpy (kJ kg⁻¹)
H	—	Total enthalpy (kW)
h_{fg}	—	Latent heat (kJ kg⁻¹)
m	—	Mass flow rate (kg s⁻¹)
p	—	Pressure (MPa); wet perimeter (m)
Q	—	Heat load (kW)
s	—	Specific entropy (kJ kg⁻¹ K⁻¹);
S	—	Concentration of seawater (g kg⁻¹); entropy rate (kJ s⁻¹ K⁻¹)
T	—	Temperature (K)

Greek

ε	—	Effectiveness of the humidifier and dehumidifier
φ	—	Relative humidity
ω	—	Humidity ratio (g kg⁻¹)

Subscripts

a	—	Air
b	—	Brine
d	—	Dehumidifier
da	—	Dry air
e	—	Exhaust
f	—	Feed
gen	—	Generation
h	—	Humidifier
$WHRE$	—	Waste heat recover exchanger
i	—	Inlet
m	—	Maximum
o	—	Outlet
r	—	Recycle
sw	—	Seawater
t	—	Total
w	—	Water

References

[1] H.F. Zheng, Solar Energy Desalination Technology. Amsterdam, Elsevier, 2017.
[2] G.H. Zhao, Z.D. Tong, Solar Energy Desalination Technology. Beijing, Chemical and Industry Press, 2011.
[3] M. Alsehli, J.K. Choi, M. Aljuhan, A novel design for a solar powered multi-stage flash desalination, Sol. Energy, 153 (2017) 348–359.
[4] P. Sharan, S. Bandyopadhyay, Solar assisted multiple-effect evaporator, J. Clean. Prod., 142 (2017) 2340–2351.
[5] J. Moumouh, M. Tahiri, M. Salouhi, L. Balli, Theoretical and experimental study of a solar desalination unit based on humidification-dehumidification of air, Int. J. Hydrogen Energ., 41 (2016) 20818–20822.

[6] J. Moumouh, M. Tahiri, M. Salouhi, Solar thermal energy combined with humidification dehumidification process for desalination brackish water: Technical review, Int. J. Hydrogen Energ., 39 (2014) 15232–15237.

[7] G. Wu, H.F. Zheng, F. Wang, Z.H. Chang, Parametric study of a tandem desalination system based on humidification dehumidification process with 3-stage heat recovery, Appl. Therm. Eng., 112 (2017) 190–200.

[8] H.F. Kang, W.N. Luo, H.F. Zheng, Z.Y. Yu, P. Cheng, Performance of a 3-stage regenerative desalination system based on humidification-dehumidification process, Appl. Therm. Eng., 90 (2015) 182–192.

[9] A.E. Kabeel, M.H. Hamed, Z.M. Omara, S.W. Sharshir, Experimental study of a humidification dehumidification solar technique by natural and forced air circulation, Energy, 68 (2014) 218–228.

[10] S.W. Sharshir, G.L. Peng, N. Yang, M.O.A. El-Samadony, A.E. Kabeel, A continuous desalination system using humidification-dehumidification and a solar still with an evacuated solar water heater, Appl. Therm. Eng., 104 (2016) 734–742.

[11] G.P. Narayan, M.H. Sharqawy, J.H. Lienhard, S.M. Zubair, Thermodynamic analysis of humidification dehumidification desalination cycles, Desal. Water Treat., 16 (2010) 339–353.

[12] O.K. Siddiqui, M.H. Sharqawy, M.A. Antar, S.M. Zubair, Performance evaluation of variable pressure humidification dehumidification systems, Desalination, 409 (2017) 171–182.

[13] Z. Rahimi-Ahar, M.S. Hatamipour, Y. Ghalavand, Solar assisted modified variable pressure humidification dehumidification desalination system, Energ. Convers. Manage., 162 (2018) 321–330.

[14] K.M. Chehayeb, Numerical fixed-effectiveness and fixed-area models of the humidification dehumidification desalination system with air extractions and injections. Master's thesis, Massachusetts Institute of Technology, 2014.

[15] B.L.D.O. Campos, A.O.S.D. Costa, E.F.D.C. Junior, Mathematical modeling and sensibility analysis of a solar humidification dehumidification desalination system considering saturated air, Sol. Energy, 157 (2017) 321–327.

[16] F.A. Al-Sulaiman, M.I. Zubair, M. Atif, P. Gandhidasan, S.A. Al-Dini, M.A. Antar, Humidification dehumidification desalination system using parabolic trough solar air collector, Appl. Therm. Eng., 75 (2015) 809–816.

[17] K.M. Chehayeb, G.P. Narayan, S.M. Zubair, J.H. Lienhard V, Thermodynamic balancing of a fixed-size two-stage humidification dehumidification desalination system, Desalination, 369 (2015) 125–139.

[18] W.F. He, F. Wu, T. Wen, Y.P. Kong, D. Han, Cost analysis of a humidification dehumidification desalination system with a packed bed dehumidifier, Energ. Convers. Manage., 171 (2018) 452–460.

[19] W.F. He, L.N. Xu, D. Han, L. Gao, Performance analysis of an air-heated humidification dehumidification desalination plant powered by low grade waste heat, Energ. Convers. Manage., 118 (2016) 12–20.

[20] K.H. Mistry, J.H. Lienhard, S.M. Zubair, Effect of entropy generation on the performance of humidification-dehumidification desalination cycles, Int. J. Therm. Sci., 49 (2010) 1837–1847.

[21] W.F. He, L. Huang, J.R. Xia, W.P. Zhu, X.K. Zhang, Y.K. Wu, Parametric analysis of a humidification dehumidification desalination system using a direct-contact dehumidifier, Int. J. Therm. Sci., 120 (2017) 31–40.

[22] G.P. Narayan, M.H. Sharqawy, E.K. Summers, J.H. Lienhard, S.M. Zubair, M.A. Antar, The potential of solar-driven humidification-dehumidification desalination for small-scale decentralized water production, Renew. Sust. Energ. Rev., 14 (2010) 1187–1201.

[23] X. Huang, Y. Li, T.F. Ke, X. Ling, W.H. Liu, Thermal investigation and performance analysis of a novel evaporation system based on a humidification-dehumidification process, Energ. Convers. Manage., 147 (2017) 108–119.

[24] E.Z. Mahdizade, M. Ameri, Thermodynamic investigation of a semi-open air, humidification dehumidification desalination system using air and water heaters, Desalination, 482 (2018) 182–198.

[25] M.H. Sharqawy, J.H. Lienhard, S.M. Zubair, Thermophysical properties of seawater: a review of existing correlations and data, Desal. Water Treat., 16 (2010) 354–380.

[26] W.D. Shen, Z.M. Jiang, J.G. Tong, Thermodynamics. Beijing, Higher Education Press, 1982.

[27] G.P. Narayan, K.H. Mistry, M.H. Sharqawy, S.M. Zubair, J.H. Lienhard, Energy effectiveness of simultaneous heat and mass exchange devices, FHMT, 023001 (2010) 1–13.

[28] G.P. Narayan, J.H. Lienhard, S.M. Zubair, Entropy generation minimization of combined heat and mass transfer devices, Int. J. Therm. Sci., 49 (2010) 2057–2066.